Effects of Point Defects on the Phase Diagram of Vortex States in High-T_c Superconductors in the $B \parallel c$ Axis

Yoshihiko Nonomura* and Xiao Hu

National Institute for Materials Science, Tsukuba, Ibaraki, 305-0047 Japan

(Received 17 November 2000)

The phase diagram for the vortex states of high-T_c superconductors with point defects in the $\vec{B} \parallel c$ axis is drawn by large-scale Monte Carlo simulations. The vortex slush (VS) phase is found between the vortex glass (VG) and vortex liquid (VL) phases. The first-order transition between this novel normal phase and the VL phase is characterized by a sharp jump of the density of dislocations. The first-order transition between the Bragg glass (BG) and VG or VS phases is also clarified. These two transitions are compared with the melting transition between the BG and VL phases.

DOI: 10.1103/PhysRevLett.86.5140 PACS numbers: 74.60.Ge, 74.25.Dw, 74.62.Dh

Vortex states in high-T_c superconductors in the $\vec{B} \parallel c$ axis have been intensively studied. Although the melting transition in pure systems has now been understood very well, experimental phase diagrams are more complicated owing to effects of impurities. In the present Letter, point defects are taken into account as the simplest impurity.

A schematic phase diagram of high-T_c vortex states with point defects is given in the inset of Fig. 1. These three phases have been observed in $YBa_2Cu_3O_{7-\delta}$ (YBCO) [1,2] and $Bi_2Sr_2CaCu_2O_{8+y}$ (BSCCO) [3,4]. The Bragg glass (BG) phase [5] is characterized by the power-law decay of correlation functions of vortex positions [5,6] and the triangular Bragg pattern of the structure factor. The vortex glass (VG) phase was first defined on the basis of phase variables [7], and can be defined alternatively on the basis of vortex positions [8]. Recent simulations including screening effects [9,10] suggest the absence of the phase-coherent VG. However, the positional VG is expected to be more stable than the phase-coherent VG [8]. Therefore, whether the VG exists as the thermodynamic phase or not is still unsettled.

The BG-VG phase boundary was studied analytically [11–13], essentially based on the Lindemann criterion. Numerically, the difference between the BG and VG phases was discussed [14–16], and the overall phase diagram was obtained recently [17,18]. However, studies based on thermodynamic quantities are still lacking.

Quite recently, another phase has been observed experimentally. Nishizaki *et al.* have found a sharp jump of the resistivity [19,20] and the magnetization [20] in optimally doped YBCO in the vortex liquid (VL) region. They pointed out that this might be the transition to the vortex slush (VS) phase [21] originally found in irradiated YBCO. The VS phase is characterized by evolution of a short-range order, and the boundary between the VS and VL phases terminates at a critical point. Similar anomalies were also observed in BSCCO [22–26].

In the present Letter, we compose the phase diagram in the pinning-strength(ϵ)-temperature(T) plane (Fig. 1) on the basis of thermodynamic quantities. The first-order melting transition occurs between the BG and VL phases as in pure systems [27,28]. A first-order transition line stretches from the melting line into the VL region dividing the VS and VL phases. The VG phase exists at much lower temperatures. The boundary between the BG and VG or VS phases is almost independent of temperature, and the phase transition is of first order. This phase diagram is quite similar to the B-T phase diagram observed experimentally.

Our formulation is based on the three-dimensional frustrated XY model on a simple cubic lattice [27,29],

$$\mathcal{H} = -\sum_{i,j\in ab\ \text{plane}} J_{ij}\cos(\phi_i - \phi_j - A_{ij}) - \frac{J}{\Gamma^2}\sum_{m,n\parallel c\ \text{axis}} \cos(\phi_m - \phi_n), \quad (1)$$

$$A_{ij} = \frac{2\pi}{\Phi_0}\int_i^j \mathbf{A}^{(2)}\cdot d\mathbf{r}^{(2)}, \qquad \vec{B} = \vec{\nabla}\times\vec{A}, \quad (2)$$

with the periodic boundary condition. Screening effects are not included in this model. A uniform magnetic field

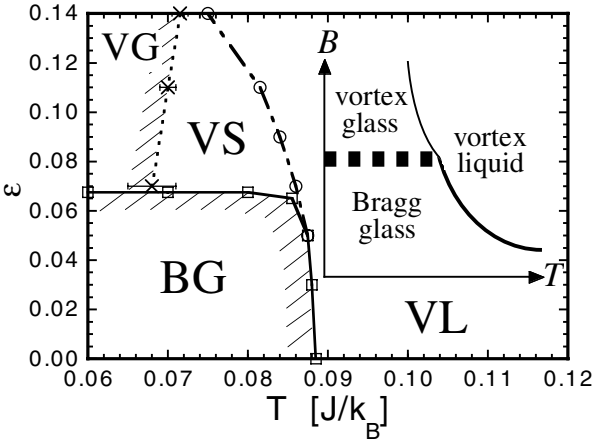

FIG. 1. ϵ-T phase diagram of the model with $\Gamma = 20$. Shaded phases exhibit superconductivity. Schematic B-T phase diagram is shown in the inset for comparison.

 0031-9007/01/86(22)/5140(4)$15.00

$\vec{B}$ is applied along the c axis, and the averaged number of flux lines per plaquette is given by $f = l^2B/\Phi_0$. Here l stands for the grid spacing in the ab plane. Point defects are introduced as the plaquettes which consist of four weaker couplings and are randomly distributed in the ab plane with probability p. Couplings are given by $J_{ij} = (1 - \epsilon)J$ $(0 < \epsilon < 1)$ on the point defects, and $J_{ij} = J$ elsewhere. Here we concentrate on the model with $\Gamma = 20$, $f = 1/25$, and $p = 0.003$. We do not consider the lower critical point [30,31] at present. The system size is $L_x = L_y = 50$ and $L_c = 40$, which is large enough to analyze the pure system ($\epsilon = 0$).

For each ϵ, Monte Carlo simulations are started from a very high temperature, and systems are gradually cooled down. After such annealing, further equilibration and measurement are performed at each temperature. Typical simulation times are $\sim(4-12) \times 10^7$ Monte Carlo steps (MCS) for equilibration, and $\sim(2-5) \times 10^7$ MCS for measurement. The present simulations are based on one sample. Since configurations of point defects are independent in different ab planes, it is reasonable to expect that there exists a self-averaging effect. We calculate the internal energy e, the specific heat C, the helicity modulus along the c axis Υ_c [27,29], and the phase difference between the nearest-neighbor ab planes $\langle\cos(\phi_n - \phi_{n+1})\rangle$, together with the ratio of entangled flux lines to total flux lines $N_{\rm ent}/N_{\rm flux}$ [28], the density of dislocations in the ab plane $\rho_{\rm d}$, and the structure factor of flux lines in the ab plane. The helicity modulus is proportional to the superfluid density, and is the order parameter of superconductivity. The interlayer phase difference is related [32] to the frequency of the Josephson plasma resonance (JPR) [33,34].

BG-VL and VS-VL phase transitions.—Temperature dependence of e, C, Υ_c, and $\langle\cos(\phi_n - \phi_{n+1})\rangle$ at $\epsilon = 0.05$, 0.07, and 0.11 is displayed in Figs. 2(a)–2(d). The BG-VL transition is observed at $\epsilon = 0.05$, and the VS-VL one at $\epsilon = 0.07$ and 0.11. Jumps of e and $\langle\cos(\phi_n - \phi_{n+1})\rangle$ and the δ-function peak of C are observed at the melting temperature $T_{\rm m}$ or the slush temperature $T_{\rm sl}$. Finite latent heats $Q = \Delta e$ indicate that these phase transitions are of first order. The anomalies of the VS-VL transition at $\epsilon = 0.07$ are as large as those of the BG-VL transition at $\epsilon = 0.05$, and gradually lose sharpness as ϵ is increased [see Figs. 2(c) and 2(d)]. At $\epsilon = 0.14$, no anomalies are observed other than a small jump of $\langle\cos(\phi_n - \phi_{n+1})\rangle$. These properties can be explained by the existence of the critical point [19–21] which terminates the first-order VS-VL transition line around $\epsilon = 0.14$.

The most important difference between the BG-VL and VS-VL transitions is seen in Υ_c. In the BG-VL transition,

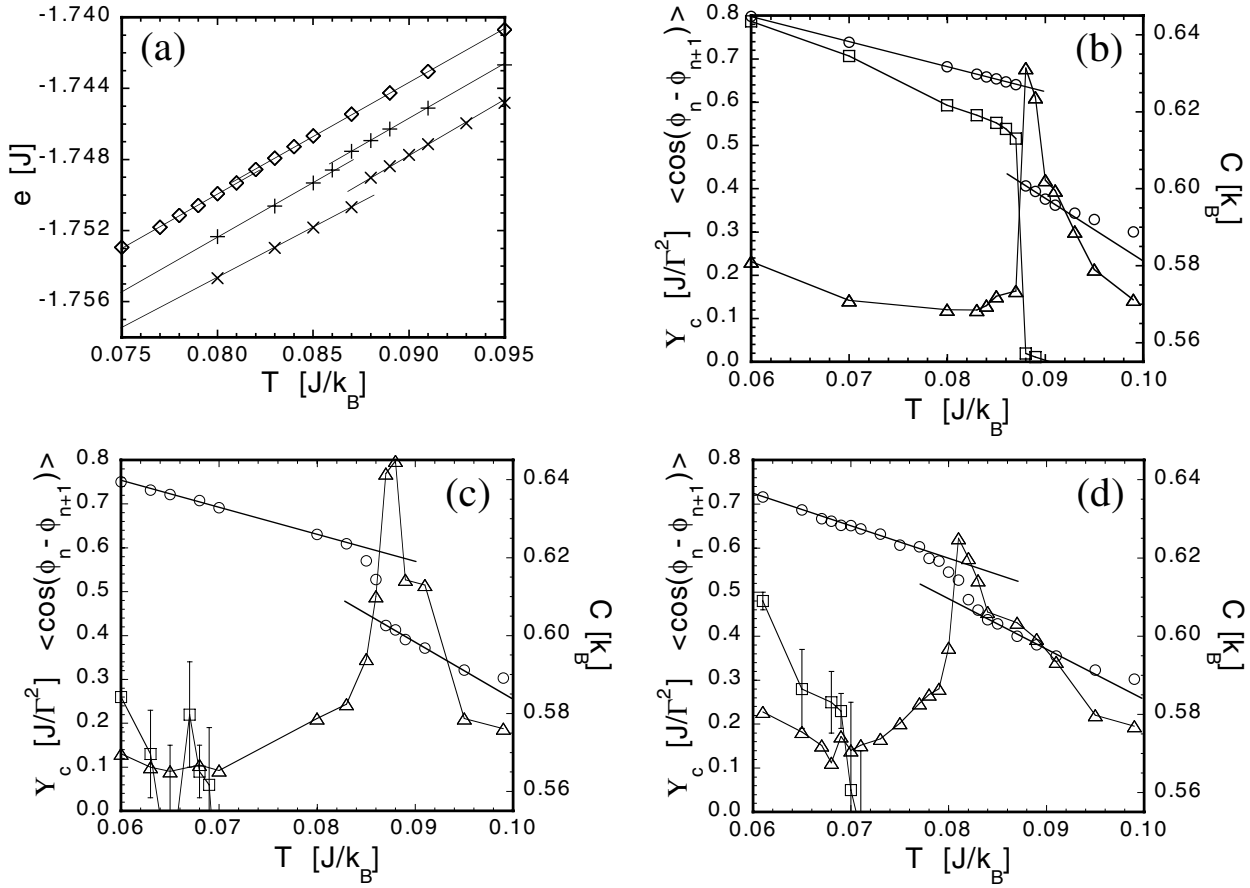

FIG. 2. Temperature dependence of (a) e at $\epsilon = 0.05$ ($\times$), 0.07 ($+$), and 0.11 ($\diamond$); C ($\triangle$), Υ_c ($\square$), and $\langle\cos(\phi_n - \phi_{n+1})\rangle$ ($\bigcirc$) at (b) $\epsilon = 0.05$, (c) 0.07, and (d) 0.11. The origin of e is varied for each ϵ in (a).

this quantity appears discontinuously at T_m. On the other hand, Υ_c remains vanishing for $T < T_{sl}$ in the VS-VL transition. In other words, the BG-VL phase transition is the superconducting-normal one, while the VS-VL transition occurs between two normal phases. The latter transition does not contradict the existence of the critical point. The proliferation of Υ_c at lower temperatures signals the phase transition to the VG phase, though error bars of Υ_c are fairly large owing to very large correlation time in the VG phase.

Direct observation of flux lines also reveals the difference between these two first-order transitions. Temperature dependence of N_{ent}/N_{flux} and ρ_d at $\epsilon = 0.05$ and $\epsilon = 0.11$ is displayed in Figs. 3(a) and 3(b), respectively. N_{ent}/N_{flux} shows a sharp jump at T_m [Fig. 3(a)] as in pure systems [28], while its temperature dependence is continuous around T_{sl} [Fig. 3(b)]. The quantity ρ_d shows sharp jumps at both T_m and T_{sl} as predicted by Kierfeld and Vinokur [35]. These properties are consistent with the structure factors shown in the same figures. A ringlike pattern is seen in the VL phase as in pure systems [27] both at $\epsilon = 0.05$ and 0.11. The clear triangular Bragg pattern for $T < T_m$ at $\epsilon = 0.05$ represents the formation of a hexatic quasi-long-range order. The obscure Bragg pattern with a sixfold symmetry for $T < T_{sl}$ at $\epsilon = 0.11$ might stand for domains of a short-range hexatic order in the ab plane divided by dislocations.

BG-VG and BG-VS phase transitions.—Pinning-strength dependence of e and $\langle\cos(\phi_n - \phi_{n+1})\rangle$ is shown in Figs. 4(a) and 4(b) for $T = 0.06J/k_B$, $0.07J/k_B$, and $0.08J/k_B$. Finite latent heats Q indicate that these phase transitions are of first order. The quantity $\langle\cos(\phi_n - \phi_{n+1})\rangle$ jumps simultaneously, which is consistent with the JPR experiment of BSCCO of Gaifullin *et al.* [36]. Since the anomalies are always observed between $\epsilon = 0.065$ and 0.070, the phase boundary is almost independent of temperature as shown in Fig. 1. We also find a sudden jump of N_{ent}/N_{flux} on this phase boundary as predicted theoretically [11,13].

The jumps of e and $\langle\cos(\phi_n - \phi_{n+1})\rangle$ (abbreviated as $\Delta\langle\cos\rangle$ from now on) on this almost-flat phase boundary are about one order smaller than those on the melting line [see Figs. 2(b) and 4(b)]. The ratio of the jump of the Josephson energy $\Delta e_J = -(J/\Gamma^2)\Delta\langle\cos\rangle$ to Q reveals the difference between these two transitions clearly. As in extremely anisotropic pure systems [37], this ratio is about one half on the melting line, e.g., $\Delta e_J \approx (5.5 \times 10^{-4})J$ and $Q \approx (1.1 \times 10^{-3})J$ at $\epsilon = 0.05$ [see Figs. 2(a) and 2(b)]. On the other hand, $\Delta e_J/Q$ is about unity on this almost-flat phase boundary, e.g., $Q \approx \Delta e_J \approx (9.0 \times 10^{-5})J$ at $T = 0.07J/k_B$ [see Figs. 4(a) and 4(b)]. The latter result shows a sharp contrast to the

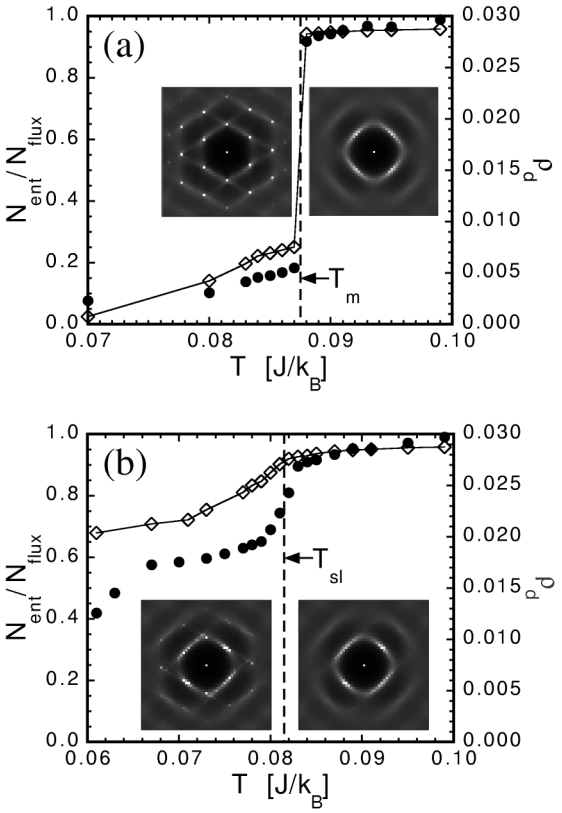

FIG. 3. Temperature dependence of N_{ent}/N_{flux} (◇) and ρ_d (•) at (a) $\epsilon = 0.05$ and (b) $\epsilon = 0.11$. Structure factors at $T = 0.087J/k_B$ and $0.088J/k_B$ are displayed in (a), and those at $T = 0.080J/k_B$ and $0.083J/k_B$ are displayed in (b).

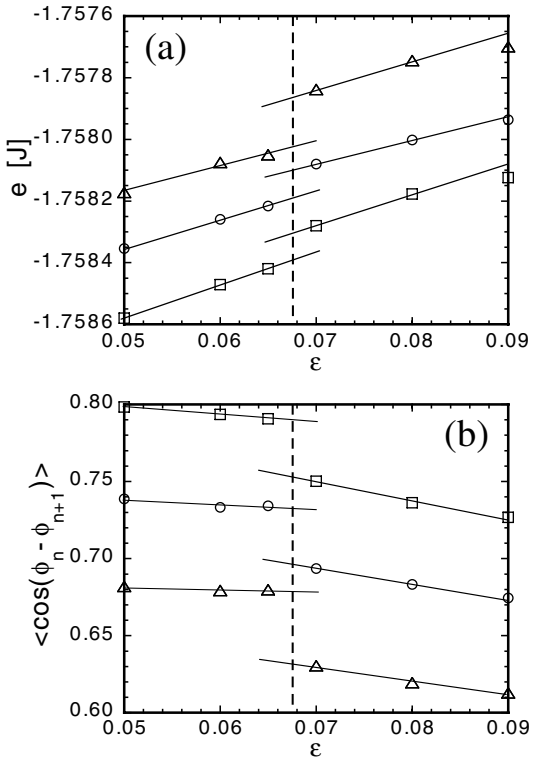

FIG. 4. Pinning-strength dependence of (a) e and (b) $\langle\cos(\phi_n - \phi_{n+1})\rangle$ at $T = 0.06J/k_B$ (□), $0.07J/k_B$ (○), and $0.08J/k_B$ (△). The origin of e is varied for each T in (a).

JPR experiment of BSCCO, where $\Delta e_J/Q \gg 1$ seems to be satisfied [38].

Discussions.—On the melting line of pure systems, $\Delta\langle\cos\rangle$ is proportional to $\Gamma^2 f$ and gradually approaches a saturated value [39], $\Delta\langle\cos\rangle \approx 0.3$ [36,40]. When the anisotropy is as small as that of YBCO ($\Gamma \approx 7$–8), $\Delta\langle\cos\rangle$ is small both on the melting line and on the BG-VG phase boundary. In the present system ($\Gamma = 20$), $\Delta\langle\cos\rangle$ (≈ 0.22 at $\epsilon = 0.05$) is as large as the saturated value on the melting line, while it is small on the BG-VG/VS phase boundary. Therefore, a jump in $\langle\cos(\phi_n - \phi_{n+1})\rangle$ inevitably occurs in the VL region, which results in the first-order VS-VL phase transition. On the other hand, when the anisotropy is as large as that of BSCCO ($\Gamma \geq 150$), $\Delta\langle\cos\rangle$ has reached the saturated value both on the melting line and on the BG-VG phase boundary as shown experimentally [36]. In such a case, it might be difficult to observe a jump of $\langle\cos(\phi_n - \phi_{n+1})\rangle$ outside of the BG phase by the JPR [38,40].

Finally, the present results summarized in Fig. 1 are compared with theoretical studies related to the VS phase in literature. When Worthington *et al.* [21] proposed the VS-VL transition line as reminiscent of the melting line in pure systems, the BG phase was out of the scope. Ikeda [41] derived a phase diagram consisting of the VG, VS, and VL phases, and argued that the BG phase and the VS phase cannot coexist. Quite recently, he modified his argument and proposed a possible phase diagram including both the BG and VS phases [42]. However, he simply assumed the existence of the BG phase in this article. Kierfeld and Vinokur [35] obtained a phase diagram consisting of the BG phase and a first-order transition line stretching from the melting line into the VL region with a critical point. Although they interpreted this transition line as the VG-VL one, it turns out to correspond to the VS-VL one as shown in the present study. Reichhardt *et al.* [43] numerically found a window-glass-like region with diverging time scales and a finite correlation length, which might also correspond to the VS phase. We believe that the present simulations are the first theoretical derivation of the phase diagram consisting of four phases (Fig. 1) based on thermodynamic quantities and from a single model. Although finite-size analyses of Υ_c [44] have not been performed at present, our system size, $L_c = 40$ for $\Gamma = 20$ and $f = 1/25$, is already very large. According to the anisotropy scaling [45], this size corresponds to $L_c \approx 113$ for the parameters in Ref. [44], $\Gamma = \sqrt{40}$ and $f = 1/20$.

We thank Y. Matsuda and T. Nishizaki for communications and A. Tanaka for comments. One of us (Y. N.) also thanks K. Kadowaki and R. Ikeda for sending their preprints. Numerical calculations were performed on Numerical Materials Simulator (NEC SX-5) at National Research Institute for Metals, Japan.

*Email address: nonomura.yoshihiko@nims.go.jp

[1] H. Safar *et al.,* Phys. Rev. B **52**, 6211 (1995).
[2] T. Nishizaki *et al.,* Phys. Rev. B **58**, 11 169 (1998).
[3] R. Cubitt *et al.,* Nature (London) **365**, 407 (1993).
[4] B. Khaykovich *et al.,* Phys. Rev. B **56**, R517 (1997).
[5] T. Giamarchi and P. Le Doussal, Phys. Rev. Lett. **72**, 1530 (1994); Phys. Rev. B **52**, 1242 (1995).
[6] T. Nattermann, Phys. Rev. Lett. **64**, 2454 (1990).
[7] D. S. Fisher *et al.,* Phys. Rev. B **43**, 130 (1991).
[8] T. Nattermann and S. Scheidl, Adv. Phys. **49**, 607 (2000).
[9] F. O. Pfeiffer and H. Rieger, Phys. Rev. B **60**, 6304 (1999).
[10] H. Kawamura, J. Phys. Soc. Jpn. **69**, 29 (2000).
[11] D. Ertaş and D. R. Nelson, Physica (Amsterdam) **272C**, 79 (1996).
[12] J. Kierfeld *et al.,* Phys. Rev. B **55**, 626 (1997).
[13] T. Giamarchi and P. Le Doussal, Phys. Rev. B **55**, 6577 (1997).
[14] M. J. P. Gingras and D. A. Huse, Phys. Rev. B **53**, 15 193 (1996).
[15] S. Ryu *et al.,* Phys. Rev. Lett. **77**, 2300 (1996).
[16] C. J. Olson *et al.,* Phys. Rev. Lett. **85**, 5416 (2000); cond-mat/0008350.
[17] A. van Otterlo *et al.,* Phys. Rev. Lett. **81**, 1497 (1998).
[18] R. Sugano *et al.,* Physica (Amsterdam) **284-288B**, 803 (2000); Physica (Amsterdam) **341-348C**, 1113 (2000).
[19] T. Nishizaki *et al.,* Physica (Amsterdam) **341-348C**, 957 (2000); see also H. H. Wen *et al.,* cond-mat/0101111.
[20] K. Shibata *et al.* (to be published).
[21] T. K. Worthington *et al.,* Phys. Rev. B **46**, 11 854 (1992).
[22] D. T. Fuchs *et al.,* Phys. Rev. Lett. **80**, 4971 (1998).
[23] T. Blasius *et al.,* Phys. Rev. Lett. **82**, 4926 (1999).
[24] B. Khaykovich *et al.,* Phys. Rev. B **61**, R9261 (2000).
[25] K. Kimura *et al.,* J. Low Temp. Phys. **117**, 1471 (1999); Physica (Amsterdam) **284-288B**, 717 (2000); Physica (Amsterdam) C (to be published).
[26] N. Chikumoto and M. Murakami, Physica (Amsterdam) C (to be published).
[27] X. Hu *et al.,* Physica (Amsterdam) **282-287C**, 2057 (1997); Phys. Rev. Lett. **79**, 3498 (1997); Phys. Rev. B **58**, 3438 (1998).
[28] Y. Nonomura *et al.,* Phys. Rev. B **59**, R11 657 (1999); J. Low Temp. Phys. **147**, 1447 (1999).
[29] Y.-H. Li and S. Teitel, Phys. Rev. Lett. **66**, 3301 (1991); Phys. Rev. B **47**, 359 (1993).
[30] M. Roulin *et al.,* Phys. Rev. Lett. **80**, 1722 (1998).
[31] L. M. Paulius *et al.,* Phys. Rev. B **61**, R11 910 (2000).
[32] L. N. Bulaevskii *et al.,* Phys. Rev. Lett. **74**, 801 (1995).
[33] M. Tachiki *et al.,* Phys. Rev. B **50**, 7065 (1994).
[34] Y. Matsuda *et al.,* Phys. Rev. Lett. **75**, 4512 (1995); **78**, 1972 (1997).
[35] J. Kierfeld and V. Vinokur, Phys. Rev. B **61**, R14 928 (2000).
[36] M. B. Gaifullin *et al.,* Phys. Rev. Lett. **84**, 2945 (2000).
[37] A. E. Koshelev, Phys. Rev. B **56**, 11 201 (1997).
[38] Y. Matsuda (private communication).
[39] Y. Nonomura and X. Hu, Physica (Amsterdam) **284-288B**, 435 (2000); Physica (Amsterdam) **341-348C**, 1305 (2000).
[40] T. Shibauchi *et al.,* Phys. Rev. Lett. **83**, 1010 (1999).
[41] R. Ikeda, J. Phys. Soc. Jpn. **65**, 3998 (1996).
[42] R. Ikeda, J. Phys. Soc. Jpn. **70**, 219 (2001).
[43] C. Reichhardt *et al.,* Phys. Rev. Lett. **84**, 1994 (2000).
[44] P. Olsson and S. Teitel, cond-mat/0012184.
[45] G. Blatter *et al.,* Phys. Rev. Lett. **68**, 875 (1992).